



Temperature activated self-lubrication in CrN/Mo₂N nanolayer coatings

Robin Abraham Koshy^{1,*}, Michael E. Graham², Laurence D. Marks³

Department of Materials Science and Engineering, Northwestern University, Evanston, IL-60201, United States

ARTICLE INFO

Article history:

Received 30 September 2008

Accepted in revised form 8 September 2009

Available online 6 October 2009

Keywords:

Lubricous oxides

Hard coatings

Lubricious oxides

High temperature lubrication

High temperature friction

Temperature activated lubrication

Multilayer coatings

CrN/Mo₂N

In-situ lubrication

Nanolayers

Multilayered coatings

Tool coatings

Self lubrication

Multi-layers

Magnetron

Sputtering

Reactive sputtering

CrN

Mo₂N

ABSTRACT

CrN/Mo₂N multilayers were deposited and TEM, SEM, EDS, XPS and TGA studies were carried out. TEM studies show crystalline layers with sharp interfaces. TGA studies indicate that the CrN protects the underlying Mo₂N layers from oxidation. On varying the periodicity the hardness of the films are in the 20–30 GPa regime, within the rule of mixtures of its constituents. Friction tests at high temperature shows the films to have a temperature activated self lubrication mechanism. Similar friction tests in a near nitrogen atmosphere shows the same temperature activated lubrication mechanism operating with the friction being in a lower regime. MoO₃ is isolated as the predominant oxides phase that evolves from the surface and at temperatures in excess of 400 °C acts as an *in situ* lubricant.

© 2009 Elsevier B.V. All rights reserved.

1. Introduction

Hard coatings for cutting tools have been in use for many decades, [1–6], and have evolved from the initial, simple nitride and oxide coatings (such as TiN and Al₂O₃) applied by CVD and PVD in the 1970s, to more complex, high-performance alloy nitrides (such as TiAlN) employed today. More recently, the interest in green manufacturing has spurred development of coatings for dry machining, [7–10]. If coatings can effectively tolerate high temperatures or can help to reduce them, then coolant usage can be reduced. If the friction level due to the cutting process can be minimized, then lubricant usage can be reduced along with power requirements. In an earlier study the authors [11] characterized the deposition conditions and bulk

properties of CrN and Mo₂N coatings and their multilayers. In this paper the intent is to describe our work to develop and characterize multilayered, CrN/Mo₂N coatings of different ratio and bi-layer periodicities. The intent is also to characterize the tribological behaviour of these coatings at high temperature and prove that CrN/Mo₂N coatings do form hard coatings that are self lubricating at high temperatures. It is proposed to use the materials in a nano-layered structure that will be hard, tough, adherent, and lubricious at the service temperature (<1000 °C). The basic system of CrN_x and MoN_x to form multi (nano)-layered coatings offers some advantages as a starting point. Cr(N) is suggested because of its excellent wear and oxidation resistance to about 800 °C, [12,13] and Mo(N) [14] because it is likely to oxidize at about 500 °C, forming its low friction oxide, MoO₃. The presumption is that the Mo-oxide will reduce the cutting friction and consequently, the heat generated by high-speed contact (relative to a coating without the Mo). Past research showed that plasma sprayed composites of Cr₂O₃ and MoO₃ benefit from the addition of MoO₃ and exhibit a reduction of sliding friction from ~.4–.5 at RT to ~.2 at 450 °C (self-mated or against Cr-plated discs) [15]. A schematic representation of the structure conceived as a self

* Corresponding author. Currently at intel. Tel.: +1 847 275 7597.

E-mail addresses: koshy@u.northwestern.edu (R.A. Koshy), mgraham@northwestern.edu (M.E. Graham), l-marks@northwestern.edu (L.D. Marks).

¹ Currently at Intel.

² Tel.: +1 847 491 5436.

³ Tel.: +1 847 491 3996.

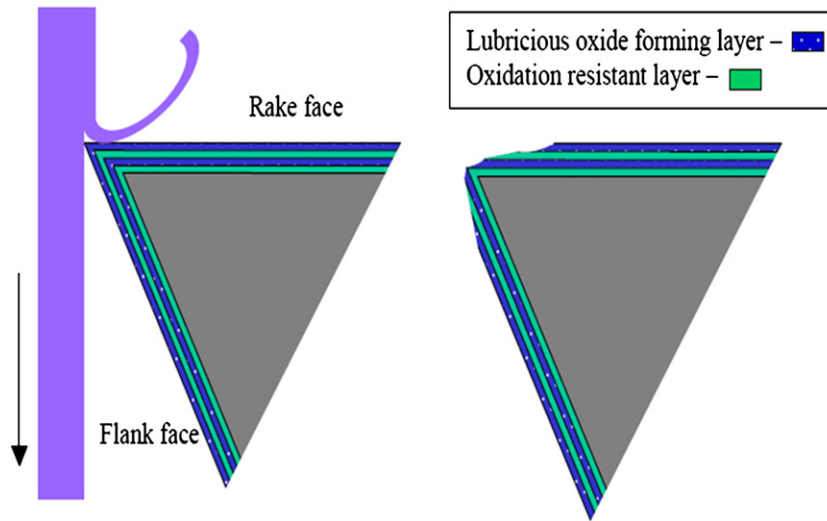


Fig. 1. Schematic representation of a cutting tool with multilayers. Alternating layers of the lubrication Mo_2N phase and the CrN phase.

lubricating tool is depicted in Fig. 1. This approach of using a lubricious oxide has also been explored by others in the cutting tool application, but they chose to explore TiO_x , [16,17], and VO_x , [18,19], as the active components. The oxide formation at temperatures above 400°C appears to offer promise for the approach. In our case, added characteristics of the selected materials are that they are both hard phases ($\sim 20\text{--}30$ GPa) and they are expected to be immiscible in their up to 800°C [20], this could result in the films retaining their layered structure (and strength) at temperatures exceeding 800°C .

2. Experimental details

The samples were prepared by sputter deposition in a closed-field dual-cathode unbalanced-magnetron system. The cryo-pumped system has a base pressure of 4×10^{-7} Torr and includes a high vacuum load lock

chamber. There are two vertically mounted $12.8\text{ cm} \times 40.6\text{ cm}$ planar magnetron cathodes facing each other on opposite sides of the substrate holder and 10 cm from the substrates. The hexagonal substrate holder is just large enough to eliminate the cross contamination from the other cathode. The substrate holder can be rotated at 5–15.2 rpm to produce nano-layered materials with controlled layer thickness. All coatings were 1–1.5 μm in total thickness. The substrates were single crystal Si (001), glass sides, and polished M50 tool steel discs ($R_a \sim 10\text{ nm}$). Sapphire substrates were used in cases where high temperature anneals were to be carried out. Prior to deposition, the samples were cleaned in an ultrasonic bath of methanol. High purity N_2 (99.99%) and Ar (ultra high purity) were used during the deposition process.

To analyze the chemical composition, XPS analysis was performed on the wear debris with an Omicron ESCA probe, which was equipped with an EA125 energy analyzer. Photoemission was stimulated by a monochromated Al K-alpha X-ray (1486.6 eV) with an operating

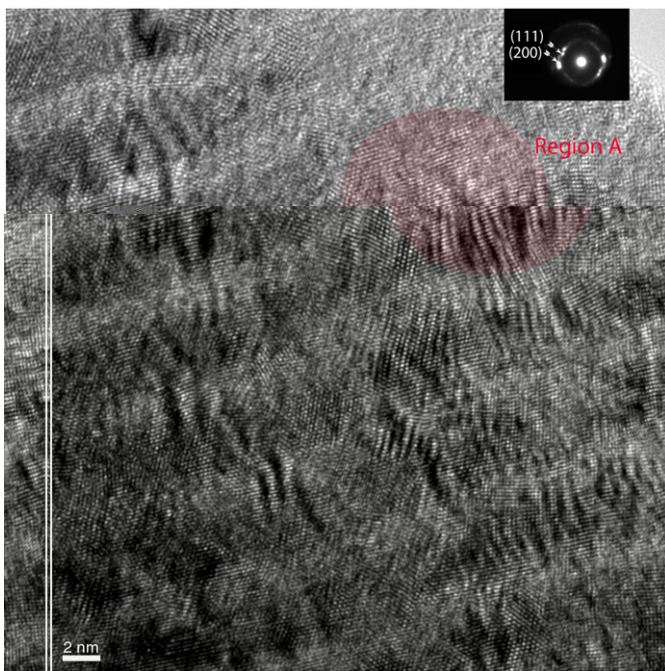


Fig. 2. Cross-section TEM micrograph of the multilayers in bright field mode. The mild contrast is due to the different phases present as well as local strains and variations in lattice orientation with respect to beam direction. The lattice ordering is also visible showing a continuity across layer boundaries (area A).

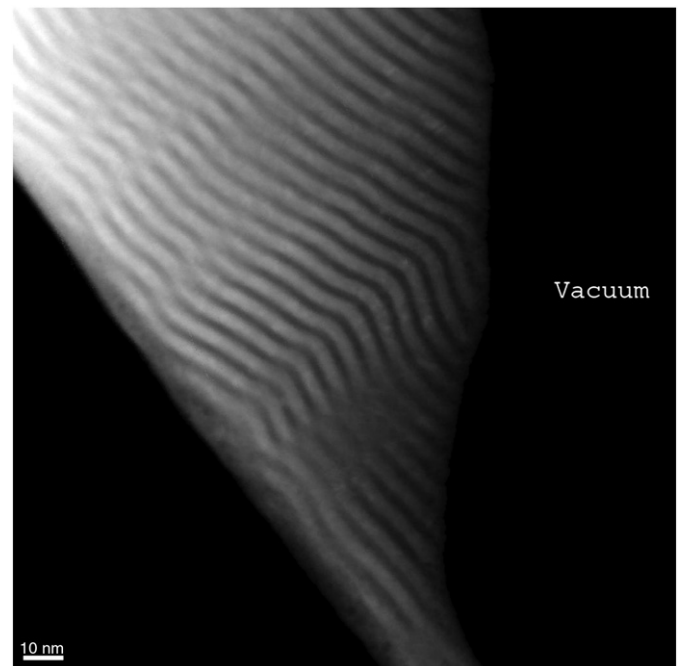


Fig. 3. Cross-section STEM micrograph of the multilayers. The sharp bright and dark contrast is due to the difference in atomic number. The brighter regions are from the heavier element (Mo) which has a high scattering angle.

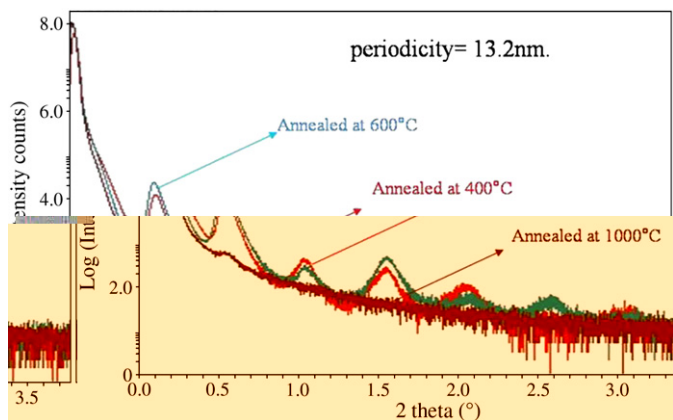


Fig. 4. Low angle X-ray diffraction of multilayer sample annealed at 400 °C, 600 °C, and 1000 °C.

power of 300 W. The analyzer was operated in the constant analyzer energy (CAE) mode at 60 eV (survey scan) and 25 eV (detailed scan) of core level lines. Binding energies were referenced to the C 1 s binding energy set at 285.0 eV. The grazing angle studies were carried out on a Rigaku AXT-G Thin-film Diffraction Workstation. The Rigaku has a high intensity 18 kW copper X-ray source coupled to a multilayer mirror. The system has selectable X-ray configurations suitable for work with single crystals. The unit also features a 5-axis goniometer with several 4-crystal monochromators that couple to the multilayer mirror.

Coating hardness was determined using a CSIRO UMIS 2000 nano-indenter fitted with a Berkovich diamond tip. The indentation depths are kept within 10% of the coating thickness. The film thickness on the Si substrate was measured using a Dektak 3030ST profilometer at the edge of a masked section of the substrate. The TGA studies were carried out in air and the mass gain was tracked with increasing temperature, where the rate of heating from room temperature was 5 °C/min and finally held at 900 °C for 15 min. The coatings were 1–1.5 μm thick and deposited on Si(100) substrates. TEM characterization was carried out on a JEOL 2100 microscope. Friction tests were carried out on a CSEM high temperature tribometer and a CETR micro-tribometer. Both the tribometers are the ball-on-disc type. All the friction tests were carried out with a 40g load at a constant sliding velocity (in rotation) of 1 cm/s, using a 3/8 inch sapphire ball. The

rate of rotation is changed to maintain a constant surface velocity for comparisons on tracks of different diameters. The COF results reported are steady state values and typical friction test durations are ~1 h. In the absence of an enclosure for our tribometer, we chose to flush the ball and race track region of our tribometer with N₂. Our friction testing in industrial grade N₂ was an attempt to eliminate O₂ from the tribometer chamber, but the industrial grade nitrogen used has trace amounts of O₂ (~5 ppm). This served to “limit” the oxidation of the surface rather than completely eliminate it. It is important to note here that being a high temperature tribometer, the presence of cooling fans makes it impossible to “completely” seal the chamber from oxygen in the air.

3. Results and discussion: CrN/Mo₂N

3.1. Deposition and characterization of CrN/Mo₂N

The key parameters the authors chose to vary here are the relative amounts of CrN and Mo₂N and the bilayer period. The first is achieved by varying the power settings on the targets. The bilayer period with a fixed CrN/Mo₂N ratio was varied by changing the rate of rotation of the substrate table. The authors have previously reported the effects of bilayer periodicity at a fixed power level [11]. The current effort explores the effects of varying the relative ratios of Cr and Mo on bulk properties and high temperature friction.

3.2. XRD, SEM and TEM analysis

Cross-section TEM analysis of the multilayer samples was carried out as shown in Fig. 2, confirming sharp interfaces in the coating. The sharp interface was also characterized by low angle X-ray diffraction and its highly crystalline structure is apparent in the TEM image. The origin of contrast in this case, in the bright field mode, of the TEM is due to the constituent layers having different atomic number (Z contrast). The lattice imaging allows us to clearly see the differences in crystal orientation across the layers of CrN and Mo₂N. The lattice mismatch between fcc-CrN and fcc-Mo₂N is ~1.5%, and as region A in Fig. 2 shows, there are some preferred orientations in the coatings that lead to epitaxy across the layers in the (111) direction. Fig. 3 shows a cross-section STEM image of the multilayer. The origin of contrast in cross-sectional STEM is almost solely due to differences in atomic number and hence, scattering angles. The STEM image

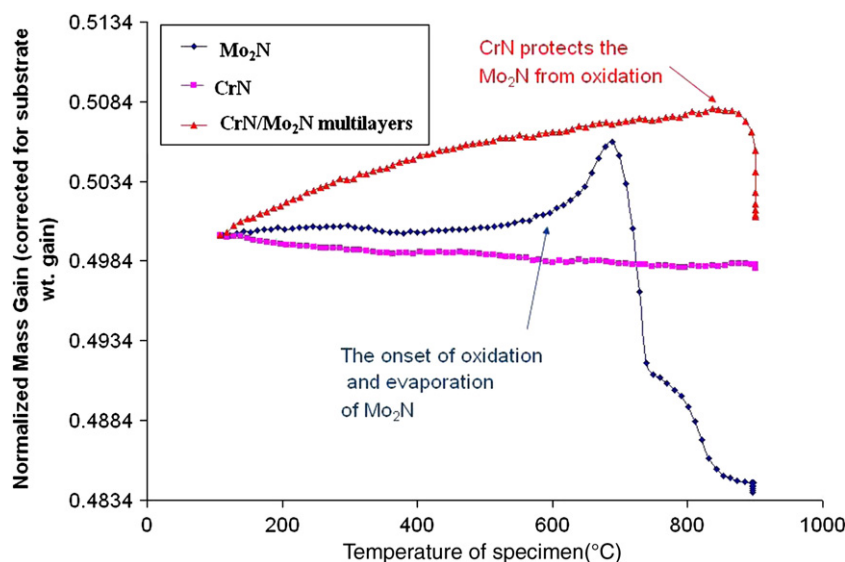


Fig. 5. TGA plots of weight gain of the substrate (Si wafer), multilayer sample (CrN/Mo₂N ::4:5), Mo₂N, and CrN.

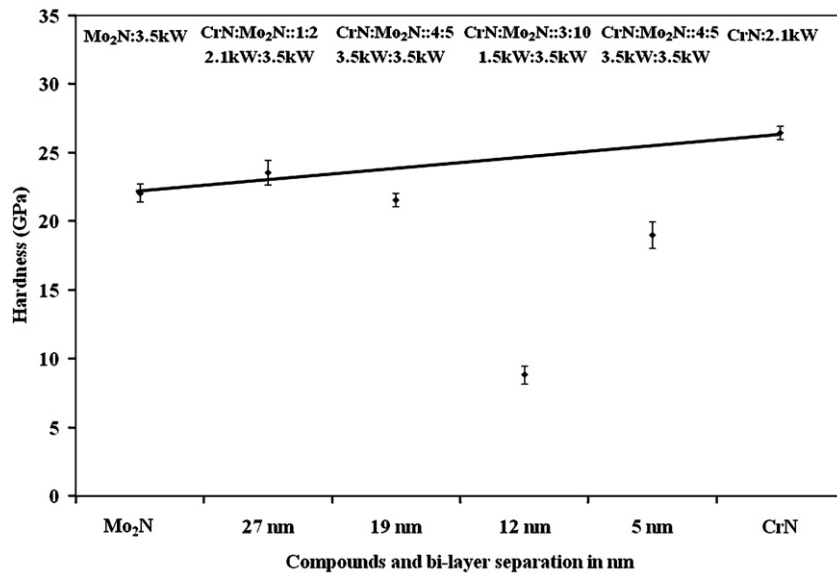


Fig. 6. Hardness of CrN and Mo₂N and the different multilayer films. The relative amounts of the phases are represented as a ratio and the power used during reactive sputtering is shown.

confirms the sharp interfaces, between non-mixing phases, which are critical to the performance of CrN/Mo₂N as a system that self lubricates at high temperature. Low angle X-ray diffraction is able to track phase modulations and as (Fig. 4) shows they are intact up to 600 °C (annealing in argon atmosphere). Since low angle X-ray diffraction studies are very sensitive to the surface roughness that developed with heating, the peaks are diminished at a 1000 °C. However, cross-section SEM images of the coating show that the layers are still present. The interface remains sharply delineated even at high temperature (1000 °C) [11]. The CrN, on oxidation, forms Cr₂O₃ at high temperature and serves as an oxidation diffusion barrier for the lower underlying layers [12,21].

3.3. TGA studies

A simple TGA study (Fig. 5) of the multilayer shows the protective nature of Cr₂O₃ formed as part of the oxidation process. The Mo₂N

bulk sample shows mass gain as early as 500 °C. At a temperature just around 700 °C there is an increased rate of oxidation indicated by mass gain, and finally at temperatures above 700 °C there is evaporation loss. The temperature regime is consistent with published results [22] for MoO₃ evaporation loss. The CrN curve on the other hand shows steady mass gain with the rise in temperature as the coating and the Si substrate oxidize [23]. It is important to note here that the coatings are deposited on a single side polished Si substrate, and the unpolished side of the substrate contributes in a substantial but deterministic way to the mass gain of the system. The most interesting of the TGA plots is the curve depicting the effects of oxidation on the multilayer system. The multilayer system shows a steady mass gain up to around 800 °C, after which there is a significant mass loss, presumably due to the loss of Mo as MoO₃. The mere presence of CrN in the multilayer and its subsequent oxidation serves to shield the lower layers from oxidation damage as it serves as a diffusion barrier [21] and delays the mass loss of Mo by 150 °C. The

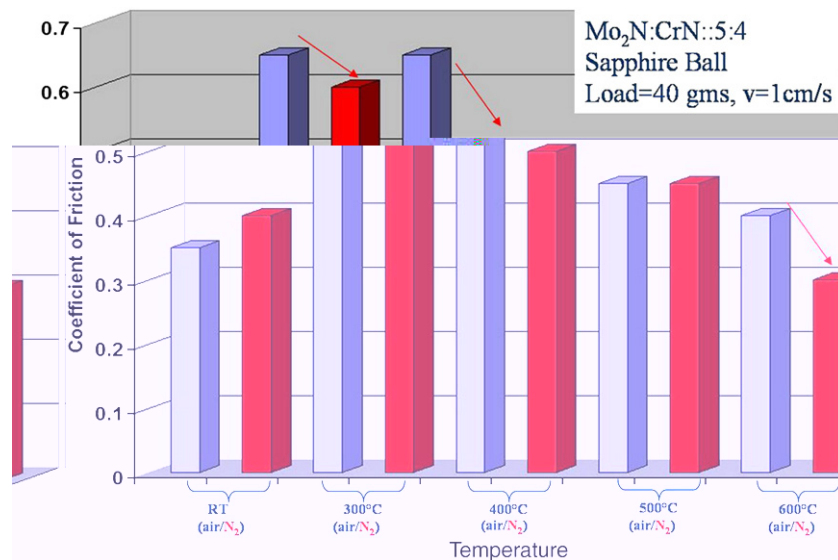


Fig. 7. High temperature friction tests of the CrN/Mo₂N ::4:5 multilayers. The friction values at a specific temperature in air and N₂ are reported side by side with air on the left hand and N₂ on the right hand side. The friction values in nitrogen are recorded when the race track and the sapphire ball region is flushed with Nitrogen.

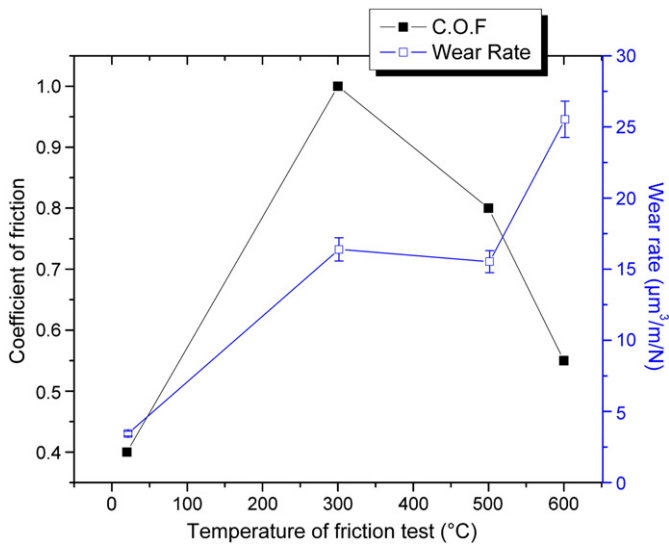


Fig. 8. Coefficient and wear rate as a function of temperature of the CrN/Mo₂N (5:4) multilayer in air.

increased mass gain of the multilayer curve over the CrN, Mo₂N or the multilayer coating is due to poor adhesion of the film to the Si wafer. This leads to the Si surface under the coating being exposed to oxidation and consequent mass gain.

3.4. Hardness analysis

As shown in Fig. 6 the relative amount of the Mo₂N is increased by varying the relative ratios of CrN/Mo₂N. The bilayer period is decreased by increasing the rate of rotation and consequently reducing the bilayer period from 19 nm to 5 nm. Our prior studies have shown that the hardness of CrN/Mo₂N multilayer coatings (when deposited at the same power level) are typically bounded by the hardness of CrN and Mo₂N.

It is important to note that the hardness of the 12 nm and 5 nm coatings is lower than the hardness of both Mo₂N and CrN specifically because the coatings were deposited at a different power level on the Cr cathode. The authors speculate that this relative softening of the

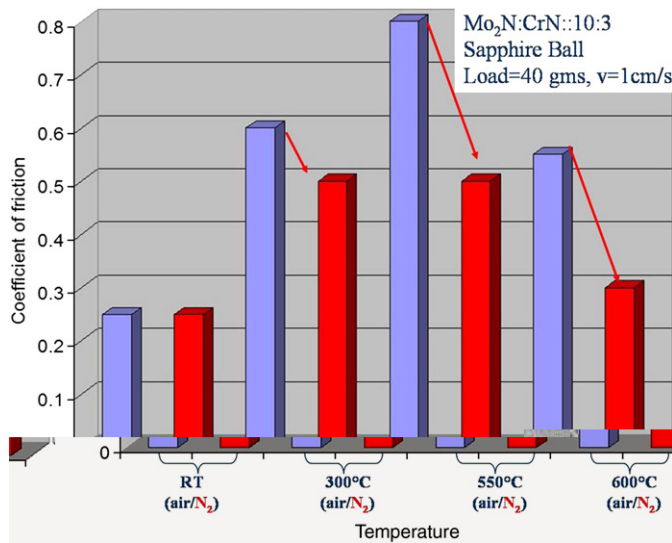


Fig. 9. High temperature friction tests of the CrN/Mo₂N ::3:10 multilayers in air. The friction values at a specific temperature in air and N₂ are reported side by side with air on the left hand and N₂ on the right hand side. The friction values in nitrogen are recorded when the race track and the sapphire ball region is flushed with Nitrogen.

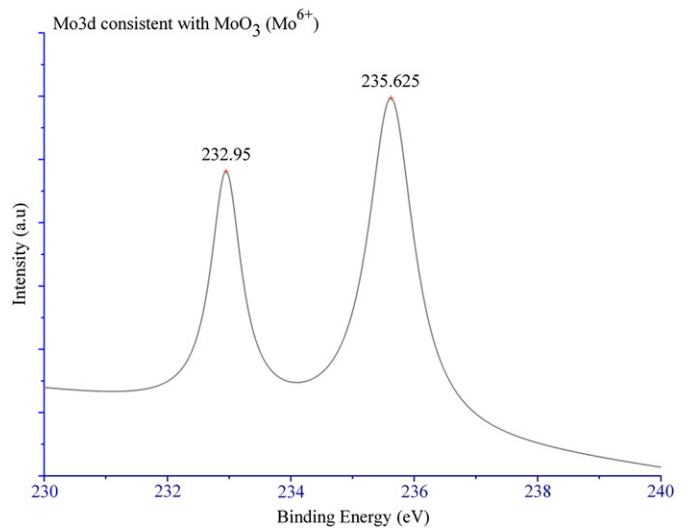


Fig. 10. Curve fitted XPS data. Analysis was carried out on wear debris collected after the test at 500 °C.

coating could be due to the lower energetic of Cr species arriving at the substrate, further testing needs to be done to directly establish the reason for this excess drop in hardness.

3.5. Friction studies on the multilayer and effect of temperature on multilayer

High temperature friction tests on the sample were carried out at a 1 cm/s, constant velocity of rotation and a 40g load. The friction values of CrN and Mo₂N tested at RT using a 52100 steel ball gave 0.7 in both cases. This was more indicative of metal on metal friction value of a highly abrasive film In Fig. 7, the CrN/Mo₂N ratio is 4:5 and the tests are carried out from RT to 600 °C close to the limits of the high temperature tribometer. As we test our sample from RT to intermediate temperatures of 300 °C there is an initial rise in friction due to the evolution of hard wear debris especially particulate CrN, Mo₂N and the highly abrasive Cr₂O₃. This immediate increase in friction is seen in all of our high temperature tests and is consistent with multilayer high-temperature tribo-tests where one of the constituents phases in the wear debris is abrasive [24,25]. (Fig. 8) shows an increase in wear rate at 600 °C. The higher wear rate is in good agreement with our findings of more transfer particles at 600 °C; this is correlated with the increase in oxidation. The wear track shows

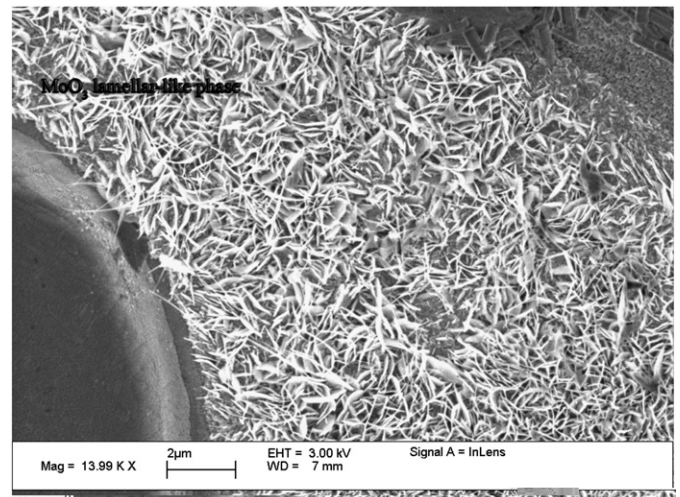


Fig. 11. SEM image of the evolution of the lamellar Mo₃ phase on the surface of the multilayer coating.

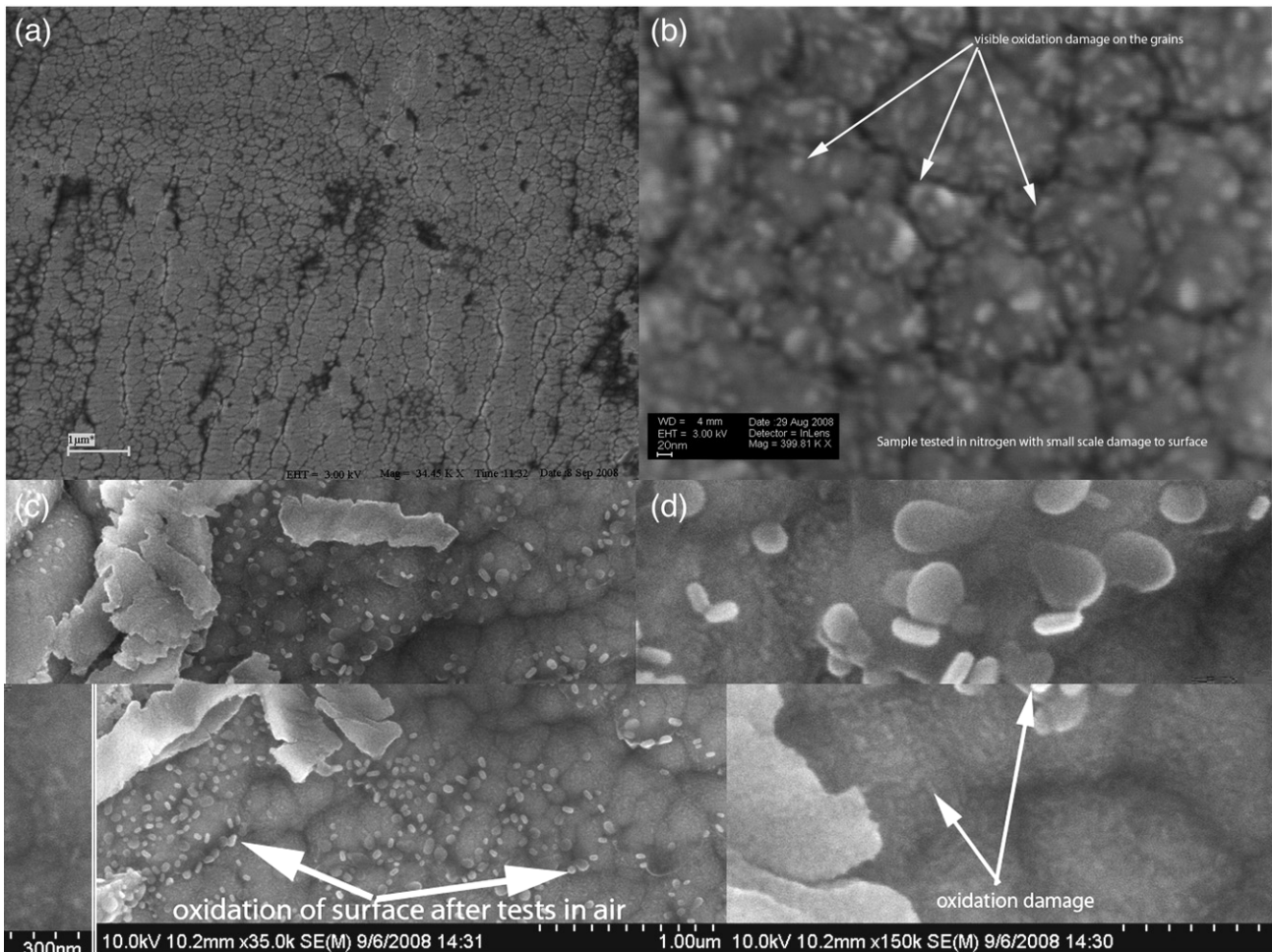


Fig. 12. SEM view of the coating surface before and after oxidation (a) as deposited (b) surface tested in nitrogen (c) surface tested in air low resolution (d) surface tested in air higher resolution.

little or no damage at room temperature, it is fair to say that temperature related damage starts at 300 °C but significantly affect the coating around 600 °C.

The authors note that in the tests carried out (CrN/Mo₂N::4:5) at 500 °C there is a friction drop associated with the generation of MoO₃, a more detailed study needs to be done to better understand how its concentration in the wear debris affects the friction.

This trend of initial friction increase and the final drop in friction is shown in our samples with a CrN/Mo₂N::3:10 (Fig. 9) as well. Based on this study the authors were not able to discern any strong dependence based on the relative ratios of CrN/Mo₂N (within the ratio range of our tests). The effects could be more pronounced at the extremes of high and low Mo and Cr concentrations in the wear debris.

3.5.1. EDS and XPS studies

The black sooty wear debris from the sapphire ball, is transferred onto a sticky carbon tape. The tape is then placed in an XPS chamber and an SEM microscope with an EDS analysis option. Subsequent XPS, (Fig. 10), and EDS studies on them revealed MoO₃ to be the predominant Mo phase of the wear debris. MoO₃ is a known low friction phase and its presence is consistent with the related drop in friction coefficient exhibited at high temperatures. As the SEM micrographs shows, MoO₃ is characterized by the growth of lamellar (plate-like) structures (Fig. 11) with increased temperature, and this is consistent with literature [22].

When the ball and race track region is flushed with nitrogen during the high temperature tests, we observed a similar trend. The friction initially increases and at temperatures of 400–500 °C there is a

drop in friction associated with the evolution of the oxides of Mo. Our XPS and SEM studies confirm the presence of Cr₂O₃ and MoO₃ in the wear debris. MoO₃ is the primary component of the wear debris. The authors find that with increasing temperature the relative amounts of the wear debris increases. This is marked by the amounts of smeared debris found in the wear track. We theorize that the relative amounts of the Cr₂O₃ and the MoO₃ determines the order of friction. The more the Cr₂O₃ in the wear debris the higher the friction and inversely the more MoO₃ in wear debris the lesser the friction. Further testing needs to be done *in situ* to confirm this.

The friction values of the high temperature tribo-test in N₂ are generally lower than the tests in air. It is important to note here that the experimental set up does not completely eliminate oxygen from the test surface, but the tests in nitrogen were carried out by flushing the testing surface with nitrogen. This only serves to lower the partial pressure of oxygen on the surface and serve as a near nitrogen atmosphere. The surface appears less damaged by the heat (Fig. 12) and devoid of large surface defects present in abundance on the samples tested in air. The oxygen partial pressure seems to limit the abrasive oxide formation (Cr₂O₃) formation in favor of MoO₃, but this dependence needs to be further investigated. The coating compares well with a few other self-lubricating coatings [26].

4. Conclusion

Multilayers of CrN and Mo₂N were deposited at different power settings and different substrate rotations to vary the relative amounts of Cr and Mo. TGA studies were carried out on the substrate to show

the temperature of evolution of the oxides and the effect of CrN protection on the multilayer coating. Consequent delay in oxidation of the MoO₃ is demonstrated. High temperature tests on the multi-layer samples shows a temperature activated self lubricating mechanism due to the oxidation of MoO₃ at high temperatures. The friction results in the near N₂ atmosphere are lower than friction results in air. XPS studies verify the presence of MoO₃ as a primary constituent of the wear debris. SEM studies point to the relative amounts of the abrasive and lubricious phases influencing the regime of the friction.

Acknowledgements

The work was supported by NSF grant award 0423419. The authors would like to thank Dr. Bob Erck and Dr. Ali Erdemir (Argonne National Labs) for help in this project. The help of Dr. Yingmin Wang and Dr. Shuyou Li is also acknowledged here. The TEM work was performed in the (EPIC) facility of NUANCE Center at Northwestern University. NUANCE Center is supported by NSF-NSEC, NSF-MRSEC, Keck Foundation, the State of Illinois, and Northwestern University.

References

- [1] P.E. Hovsepian, W.D. Munz, *Vacuum* 69 (2002) 27.
- [2] J. Patscheider, T. Zehnder, M. Diserens, *Surf. Coat. Technol.* 146 (2001) 201.
- [3] A. Erdemir, M. Halter, G.R. Fenske, *Wear* 205 (1997) 236.
- [4] A.A. Voevodin, J.S. Zabinski, *Thin Solid Films* 370 (2000) 223.
- [5] K.L. Strong, J.S. Zabinski, *Thin Solid Films* 406 (2002) 174.
- [6] E. Lugscheider, O. Knotek, K. Bobzin, S. Barwulf, *Surf. Coat. Technol.* 133 (2000) 362.
- [7] S. PalDey, S.C. Deevi, *Mater. Sci. Eng., A Struct.* 342 (2003) 58.
- [8] W.D. Munz, *J. Vac. Sci. Technol., A* 4 (1986) 2717.
- [9] A. Horling, L. Hultman, M. Oden, J. Sjolen, L. Karlsson, *J. Vac. Sci. Technol., A* 20 (2002) 1815.
- [10] J. Musil, H. Hruby, *Thin Solid Films* 365 (2000) 104.
- [11] R.A. Koshy, M.E. Graham, L.D. Marks, *Surf. Coat. Technol.* 202 (2007) 1123.
- [12] S. Hofmann, H.A. Jehn, *Werkst. Korros.* 41 (1990) 756.
- [13] P. Hones, R. Sanjines, F. Levy, *Surf. Coat. Technol.* 94–5 (1997) 398.
- [14] P. Hones, N. Martin, M. Regula, F. Levy, *J. Phys., D, Appl. Phys.* 36 (2003) 1023.
- [15] I.W. Lyo, H.S. Ahn, D.S. Lim, *Surf. Coat. Technol.* 163 (2003) 413.
- [16] T. Aizawa, A. Mitsuo, S. Yamamoto, T. Sumitomo, S. Muraishi, *Wear* 259 (2005) 708.
- [17] A. Mitsuo, S. Uchida, S. Yamamoto, T. Aizawa, *Surf. Coat. Technol.* 188–89 (2004) 630.
- [18] G. Gassner, P.H. Mayrhofer, K. Kutschej, C. Mitterer, M. Kathrein, *Tribol. Lett.* 17 (2004) 751.
- [19] R. Franz, J. Neidhardt, B. Sartory, R. Kaindl, R. Tessadri, P. Polcik, V.H. Derflinger, C. Mitterer, *Tribol. Lett.* 23 (2006) 101.
- [20] M. Venkatraman, J.P. Neumann, *ASM Handbook, Alloy Phase Diagrams*, 1992, p. 2.155.
- [21] P. Kofstad, K.P. Lillerud, *J. Electrochem. Soc.* 127 (1980) 2410.
- [22] Z.W. Li, Y.D. He, W. Gao, *Oxid. Met.* 53 (2000) 577.
- [23] D.B. Lee, Y.C. Lee, S.C. Kwon, *Surf. Coat. Technol.* 141 (2001) 227.
- [24] T. Suszko, W. Gulbinski, J. Jagielski, *Surf. Coat. Technol.* 200 (2006) 6288.
- [25] M. Suzuki, M. Moriyama, M. Nishimura, M. Hasegawa, *Wear* 162 (1993) 471.
- [26] R.A. Koshy, Ph.D Thesis, Northwestern University, 2008.